Shadowing instability in three dimensions

Jian Hua Yao and Hong Guo
Centre for the Physics of Materials, Department of Physics, McGill University, 3600 University Street, Montreal, Quebec, Canada H3A 2T8
(Received 23 September 1992)

We study a nonequilibrium interface growth model that includes the nonlocal shadowing effect in three spatial dimensions. The model is represented by a stochastic partial differential equation for the local growth rate of an interface. The nonlocal effect is modeled by a term in the growth rate that is proportional to the local exposure angle. This leads to a shadowing instability, and the interface develops into a mountain landscape which coarsens in time. The structure factor of the interface shape shows a dynamic scaling form. The scaling exponents are computed.

PACS number(s): 05.70.Ln, 05.40+j, 64.60.Ht, 68.35.Fx

The physics associated with the formation and evolution of dynamic structures has attracted considerable interest in both experimental and theoretical studies [1]. In the simplest-pattern formation problems, there exists a moving interface between two phases, a vapor and a solid or a liquid, or two liquids, on which competing stabilizing and destabilizing forces act. The stabilizing force is usually provided by interfacial tension or stiffness, or by surface diffusion of particles. These tend to make the interface smooth. The destabilizing force can be generated by, say, an incoming particle beam, or a latent heat flux. It is the interplay between these forces which controls the dynamical evolution of the interfacial pattern. Specific systems that have received much attention over the last several years include viscous fingering in a Hele-Shaw cell [2, 3], dendritic growth of a solid from a melt [1, 3, 4], and directional solidification [1]. Center to these systems is the presence of the Mullins-Sekerka instability that makes the advancing interface unstable against long wavelength fluctuations [5], thus leading to the development of interfacial patterns from the initially flat shape. The full dynamic evolution of an unstable interface caused by Mullins-Sekerka instability in the case of a linear Hele-Shaw flow has recently been studied [6, 7].

While interface instabilities in systems such as the Hele-Shaw flow, dendritic growth, and directional solidification have largely been understood, there are other similar but different instabilities that happen in interface systems far from equilibrium and have received less attention so far. Consider the following situation of particles being randomly deposited onto a substrate for the growth of a thin film. Since the particles arrive on the surface at random positions, small undulations of the surface height may occur. If the particles strike the substrate from random angles, peaks of the surface undulation may receive more incoming material, and thus grow faster than the average growth rate. Meanwhile, valleys of the surface undulation will be deprived from the material since they are screened or shadowed by the peaks; therefore, they grow slower than the average. This may lead to an instability on the surface such that a mountain landscape or columnar structure develops in time, and the film becomes extremely rough. In a recent article, Karunasiri, Bruinsma, and Rudnick studied this shadowing instability in the context of thin film growth by sputtering [8], in $1+1$ dimensions. In their model, the local growth rate of the interface height $h(\mathbf{r},t)$ is proportional to the exposure angle $\Omega(\mathbf{r},\{h\})$ (see below) that measures how much "sky" that one can see at position $\mathbf{r}$. Obviously Ω is nonlocal since it is a functional of the interface shape $h(\mathbf{r},t)$. For the stabilizing effect they considered the mechanism of surface diffusion. Finally a stochastic term is also included which mimics all the fluctuating effects. This model indeed generated extremely rough surface structures which are grasslike [9].

The importance of shadowing effects in sputter deposition has previously been recognized. In a series of studies, Krug and Meakin [10] investigated ballistic deposition where particles move toward the growing substrate in a direction different from the normal. On the other hand, some groups [11, 12] have argued that growth in sputter deposition proceeds according to the Huygens principle, familiar from optics. This model is believed to be valid for the peak region of the mountain landscape if noise is negligible.

Recently we have extended the model of Karunasiri, Bruinsma, and Rudnick to include the effects of desorption and lateral growth [13] and explored the possibility of studying the shadowing instability using microscopic models [14]. In these studies, it was found that the columnar structure coarsens while growing, and the coarsening of the structure obeys a dynamic scaling in which the power spectrum of the interface shape can be written as

$$P(\mathbf{k},t) \equiv \langle |h(\mathbf{k},t)|^2 \rangle \sim (t-t_0)^{\delta} F\big(k(t-t_0)^{p}\big) , \quad (1)$$

where $h(\mathbf{k},t) = \sum_i [h(\mathbf{r}_i,t) - \overline{h}(t)] \exp(i\mathbf{k}\cdot\mathbf{r}_i)/L^d$, $\langle\,\rangle$ and the overbar denote an ensemble average over the random noise and space, respectively. t_0 is some reference time that equals zero in the studies of Ref. [13] in $1+1$ dimensions. The exponent p measures the coarsening of the structure, i.e., the average radius of the cross section of the columns $\zeta(t)$ grows as a power law $\zeta(t) \sim t^p$. The value of p is different for the two models studied in Ref. [13], but is between zero and one in $1+1$ dimensions. Ex-

periments on silicon carbide films are consistent with an exponent [15] $p \approx 0.2$ to 0.73 for high and low termperatures, respectively. Furthermore, if $W(t)$ is the interface width defined as $W^2(t) \equiv \sum_i [h(\mathbf{r}_i,t) - \overline{h}(t)]^2/L^d$, where $d+1$ is the full spatial dimensions, the identity $W^2(t) \equiv \int P(\mathbf{k},t)d\mathbf{k}$ provides a scaling relationship between the two exponents δ and p,

$$\delta = 2\beta + dp \ , \tag{2}$$

where we assumed a power law time dependence [16] $W(t) \sim t^\beta$. This scaling relationship is indeed satisfied by our model in $1+1$ dimensions [13].

The purpose of this paper is to report further studies of the shadowing instability in $2+1$ dimensions. We are not aware of any $(2+1)$-dimensional studies in the literature on this subject presumably due to computational difficulties since the instability is caused by the long-range screening effect. As we may see below the computational effort is increased considerably compared with that of the $(1+1)$-dimensional calculations. Our model is represented by the following stochastic partial differential equation for the interface height variable:

$$\frac{\partial h}{\partial t} = \nu \nabla^2 h + R\Omega(\mathbf{r},\{h\}) + \eta \ , \tag{3}$$

where ν and R are constants. The first term on the right-hand side represents the evaporation dynamics that we take as the dominant annealing mechanism for surface relaxation. The last term is the combined effect of short noise and thermal noise of the substrate, which we assume satisfies a Gaussian statistics, $\langle \eta(\mathbf{r},t)\rangle = 0$, and $\langle \eta(\mathbf{r},t)\eta(\mathbf{r}',t')\rangle = 2D\delta(\mathbf{r}-\mathbf{r}')\delta(t-t')$, where D is a constant. The nonlocal term $R\Omega(\mathbf{r},\{h\})$ in (3) is the growth rate at location $\mathbf{r}$ of the growing surface, where Ω is the exposure angle at $\mathbf{r}$ (see below). For the $(2+1)$-dimensional interface this is a solid angle. The motivation of this term is obvious: a higher location on the interface should receive more incoming particles than a lower location. In general, higher places correspond to larger values of $R\Omega(\mathbf{r},\{h\})$. Therefore, this term represents a simple way to mimic the shadowing effects [17]. To ensure that the total incoming particle flux is a constant throughout the growth, the equation is subjected to a constraint,

$$\int_0^L d\mathbf{r}\Omega(\mathbf{r},\{h\}) \ = \ L^d \ . \tag{4}$$

We note that if the dominant annealing mechanism is surface diffusion, the linear term of (3) will be $-D\nabla^4 h$, as discussed above and studied in Ref. [8]. Finally it is important to note that (3) can only be used to study interface dynamics of amorphous materials, since faceting effects are neglected completely.

To see that (3) has an intrinsic instability, a linear stability analysis can be performed [8]. Take a flat interface which lies in the x-y plane and is perturbed by a sine profile in, say the x direction, then $h(\mathbf{r},t) = h_0 \sin(kx)\exp(\omega_k t)$ where h_0 is small. For this profile and small h_0, the exposure angle $\Omega(\mathbf{r},\{h\})$ can be computed to be linear in h_0 as $\Omega \approx \overline{\Omega} + \alpha k h_0 \sin(kx)$, where $\alpha \approx 0.11$. From Eq. (3) we then obtain a dispersion relation

$$\omega_k = \alpha R k - \nu k^2 \ . \tag{5}$$

Thus the modes with $k < k_c = \alpha R/\nu$ are unstable ($\omega_k > 0$) and grow in time, whereas the modes with $k > k_c$ decay in time ($\omega_k < 0$) and are annealed away. This instability results from the competition between the desorption and shadowing effects. Away from the linear regime, there is little hope to solve Eq. (3) analytically, and we have thus integrated it numerically.

The numerical solution of Eq. (3) is quite tricky in $2+1$ dimensions. The difficulty comes from the evaluation of the exposure angle Ω. To compute this quantity, we have discretized Eq. (3) on an $L \times L$ grid. For each grid point (x,y), the azimuthal angle ϕ is also discretized into M slices, and the polar angle $\theta(\phi)$ is computed for each of these slices using a method similar to that of $1+1$ dimensions [13]. The inset of Fig. 2 is a sketch of the polar angle $\theta(\phi_i)$ on the interface for a particular azimuthal angle ϕ_i. Finally the exposure angle Ω is computed from

$$\Omega(\mathbf{r},\{h\}) \approx \sum_{i=1}^{M} \delta\phi_i \int_0^{\theta(\phi_i)} \sin\theta' d\theta' \ , \tag{6}$$

where $\delta\phi_i = 2\pi/M$. In our calculations, we have fixed M to be 48. This algorithm demands a computation of the order $O(L^4)$ for each time step of the iteration, and this is a major limitation of the system sizes that one can use. In particular, we have used $L = 96$. A Euler scheme is used for the time integration of Eq. (3) with a time step $\delta t = 0.025$ which we find to be small enough for reasonable accuracy. For the data presented below, a total of 10 000 time steps were integrated with initial interfaces being flat. For each set of parameters, 10 independent runs were averaged [18]. Finally, we note the necessity of the constraint (4): without it the flux of the incoming particle beam would change in time in an unpredictable manner and is thus unphysical. In order to let $\Omega(\mathbf{r},\{h\})$ satisfy (4), we have scaled Ω by its average value in each time step.

Figure 1 shows the interface profiles at 3500, 7000, and 10 000 time steps for parameters $\nu = 0.3$, $R = 1.0$, and $D = 0.0005$. With these parameters and system size, unstable modes are present in the system and the initially flat interface becomes unstable against small perturbations due to the noise term. As time increases, the unstable modes grow and eventually dominate the noise [13]. As a result, a mountain landscape develops with many peaks and valleys. Due to the screening effect larger peaks grow faster than smaller peaks, while valleys grow extremely slowly since they are deprived from the incoming particles. This process leads to a coarsening of the structure.

The mountain landscape is exceedingly rough with very large undulations on the interface. The roughness can be monitored by the growth of the interface width $W(t)$. Similar to other unstable interfaces, such as in the problem of viscous fingering [6, 7] or in our earlier study on a $(1+1)$-dimensional system, here $W(t)$ is a linear

function of time t after a brief initial transient [19]. This is shown in Fig. 2 for two different values of ν. The linear dependence on time directly indicates the presence of an instability: the peaks are growing, while the valleys are almost held stationary. For larger ν the surface relaxation is faster and the instability comes at later time.

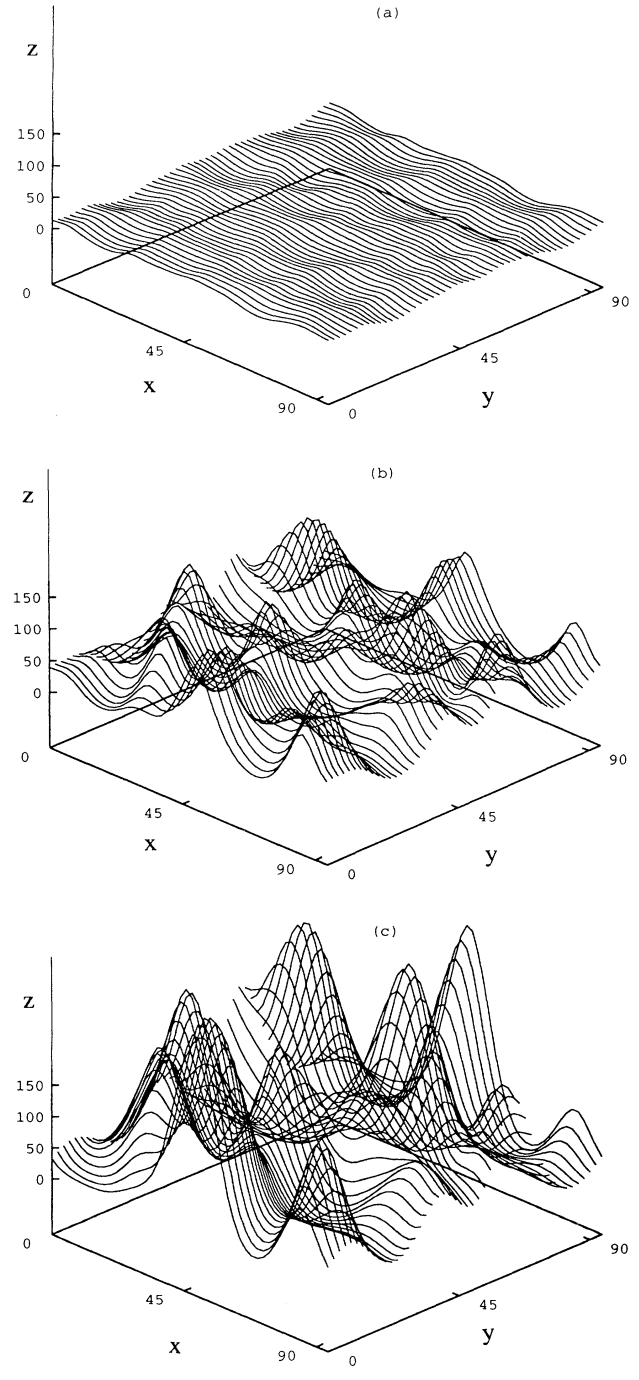

FIG. 1. Interface profiles at (a) 3500, (b) 7000, and (c) 10 000 time steps for parameters $\nu = 0.3$, $R = 1$, and $D = 0.0005$. The initial profile is flat. The linear system size is $L = 96$.

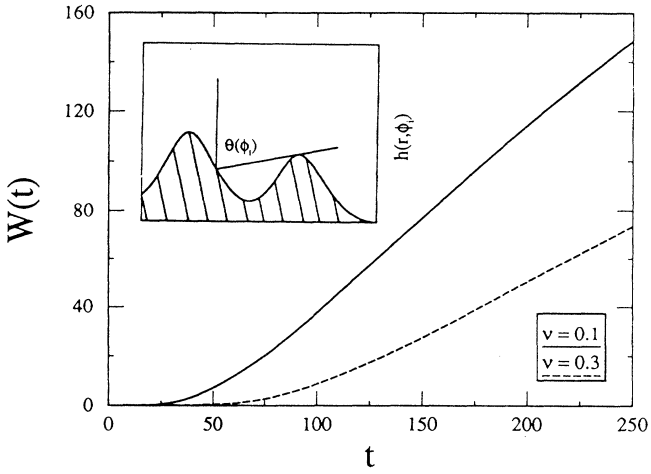

FIG. 2. The inset shows a sketch of a cut on the three-dimensional system showing the polar angle $\theta(\phi_i)$ that contributes to the calculation of the exposure angle Ω, for a particular azimuthal angle ϕ_i. The two curves show interface width $W(t)$ vs time t for two different values of ν. Other parameters are the same as those in Fig. 1.

Indeed, Fig. 2 shows that for $\nu = 0.3$ the linear dependence of $W(t)$ on t comes later in time as compared with that of $\nu = 0.1$.

The coarsening of the surface structure is best studied by monitoring the power spectrum of the surface shape, Eq. (1), as a function of time. It is convenient to introduce the circularly averaged power spectrum since our system is isotropic in the x-y plane, $P(q,t) = (1/N_k)\sum_{\mathbf{k}} P(\mathbf{k},t)$, where $P(\mathbf{k},t)$ is computed from the Fourier transform of the interface shape, as in (1). The sum is over all $N_{\mathbf{k}}$ modes such that $|\mathbf{k}|$ lies between $q-\Delta q/2$ and $q+\Delta q/2$ with $\Delta q = 2\pi/L$. The inset of Fig. 3(b) shows $P(q,t)$ as a function of wave vector q for different times. A peak clearly exists at a finite q value and it shifts to lower values of q as time increases, indicating the presence of a coarsening process. The scaling property of $P(q,t)$ was studied using (1). The two exponents p and δ were obtained by adjusting one of them, say p, and using the scaling relation (2) for the other, until all data collapse onto a single curve. We note that the derivation [13] of the relation (2) relies on the fact that the width $W(t)$ is linear in t. Here $W(t)$ only becomes linear in t after some initial transient t_0; see Fig. 2. Thus we have used a finite t_0 in fitting the scaling ansatz (1). Figure 3 shows the scaling function $F(q(t-t_0)^p)$ obtained using $p = 0.33 \pm 0.02$ and $\delta = 2.66 \pm 0.04$. Good data collapsing is obtained indicating that the dynamic scaling (1) is obeyed. We conclude that the power law coarsening of the transverse length scale, $\zeta(t) \sim t^p$, holds in 2+1 dimensions within this model. Finally, this behavior is independent of system parameters used as Figs. 3(a) and 3(b) have shown.

It is interesting to compare the findings here to those of 1 + 1 dimensions [13]. The shape of the linear stability dispersion relation in 1 + 1 dimension is different in that it has more unstable modes [20], thus the initial

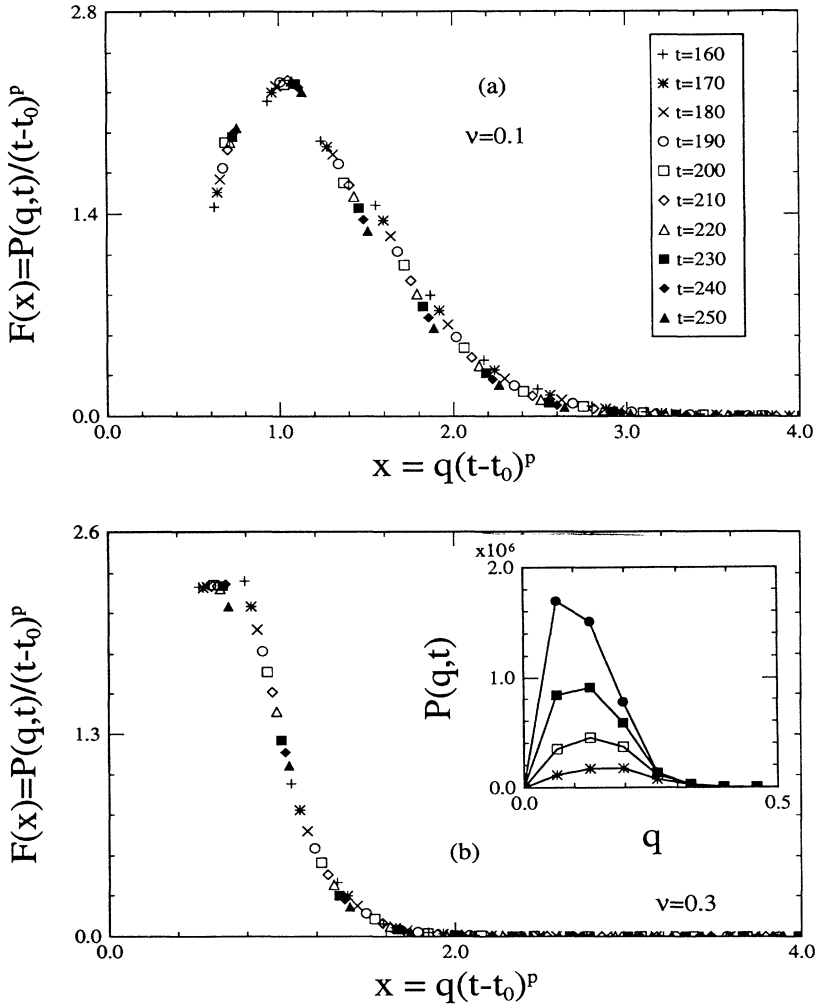

FIG. 3. Scaling plots of the power spectrum using $\delta = 2.66$ and $p = 0.33$. Data with wave numbers n from 2 to 48 are used. The wave vector $q = (2\pi/L)n$. Different symbols represent different times as indicated. The parameter $\nu = 0.1$ and $t_0 = 47.2$ for (a); $\nu = 0.3$ and $t_0 = 91.6$ for (b). Other parameters are the same as those of Fig. 1. The inset in (b) shows the circularly averaged power spectrum $P(q,t)$ as a function of wave vector q for different times. The peak moves to lower values in q indicating coarsening.

interface undulations grow faster in time. In Ref. [13] we studied Eq. (3) with an extra term $\lambda(\nabla h)^2$ that accounts for the lateral growth effects. With finite λ the coarsening exponent $p = 1$ in $1+1$ dimension. We have checked that this value drops to $\sim$ 0.7 with $\lambda = 0$ in the same dimension. In $2+1$ dimensions, the linear size of the coarsening columnar structure has a growth exponent $p \approx 0.33 \pm 0.02$ as mentioned above, so that the cross section of the structure grows, on average, with an exponent $2p \approx 0.66 \pm 0.04$. This value being close to that of the $1+1$ dimension (within error) implies that the weaker shadowing effects in $2+1$ dimensions only change the coarsening prefactor of the structure, not the exponent. This is, indeed, rather surprising.

In conclusion, we have studied the consequences of long range shadowing effects on the interfacial dynamics far from equilibrium in $2+1$ dimensions. Such effects are important in determining the surface morphology in the growth of thin films. The model we have studied is an extension of the work of Karunasiri, Bruinsma, and Rudnick [8], but we have focused on the dynamic scaling behavior of the growing surface. We have also taken desorption as the dominating surface relaxation mechanism, instead of surface diffusion. Shadowing leads to an instability on the interface such that a mountain landscape or columnar structure develops, which coarsen in time with a dynamic scaling. In particular, the length scale associated with the coarsening grows with a power law in time. This agrees qualitatively with some experimental findings [15].

We would like to thank Dr. C. Roland and Dr. J. Wang for useful discussions. H.G. has benefited from conversations with Dr. J. Krug and Dr. S. Bales. This work was supported by the Natural Sciences and Engineering Research Council of Canada, and le Fonds pour la Formation des Chercheurs et l'Aide à la Recherche de la Province du Québec.

[1] See, for example, articles included in *Dynamics of Curved Fronts*, edited by P. Pelcé (Academic, Boston, 1988).
[2] P.G. Saffman and G.I. Taylor, Proc. R. Soc. London, Ser. A **245**, 312 (1958); P.G. Saffman, J. Fluid Mech. **173**, 73 (1986).
[3] J.S. Langer, in *Chance and Matter*, Proceedings of the Les Houches Summer School Session, Vol. 46, edited by J. Souletie, J. Vannimenus, and R. Stora (North-Holland, Amsterdam, 1986).
[4] D. Kessler, J. Koplik, and H. Levine, Adv. Phys. **37**, 255 (1988).
[5] W.W. Mullins and R.F. Sekerka, J. Appl. Phys. **34**, 323 (1963).
[6] D. Jasnow and J. Viñals, Phys. Rev. A **41**, 6910 (1990).
[7] H. Guo, D.C. Hong, and D.A. Kurtze, Phys. Rev. A **46**, 1867 (1992); see also H. Guo and D. Jasnow, Phys. Rev. B **34**, 5027 (1986).
[8] R.P.U. Karunasiri, R. Bruinsma, and J. Rudnick, Phys. Rev. Lett. **62**, 788 (1989); **63**, 693 (1989).
[9] G.S. Bales, R. Bruinsma, E.A. Eklund, R.P.U. Karunasiri, J. Rudnick, and A. Zangwill, Science **249**, 264 (1990).
[10] J. Krug and P. Meakin, Phys. Rev. A **40**, 2064 (1989); **43**, 900 (1991); P. Meakin and J. Krug, Europhys. Lett. **11**, 7 (1990); see also P. Meakin and R. Jullien, Phys. Rev. A **41**, 983 (1990); J. Krug (unpublished).
[11] G.S. Bales and A. Zangwill, Phys. Rev. Lett. **63**, 692 (1989).
[12] C. Tang, S. Alexander, and R. Bruinsma, Phys. Rev. Lett. **64**, 772 (1990).
[13] J.H. Yao, C. Roland, and H. Guo, Phys. Rev. A **45**, 3903 (1992).
[14] C. Roland and H. Guo, Phys. Rev. Lett. **66**, 2104 (1991).
[15] For some experimental studies, see R.A. Roy and R. Messier, Mater. Res. Soc. Symp. Proc. **38**, 363 (1985); B.A. Mouchan and A.V. Denchishin, Phys. Mat. Metallog. **28**, 83 (1969); R. Messier and J.E. Yehoda, J. Appl. Phys. **58**, 3739 (1985); J.E. Yehoda and R. Messier, Appl. Surf. Sci. **22/23**, 590 (1985); R.A. Roy and R. Messier, J. Vac. Sci. Technol. **2**, 312 (1984); R. Messier, A.P. Giri, and R.A. Roy, *ibid.* **2**, 500 (1984).
[16] F. Family and T. Vicsek, J. Phys. A **18**, L75 (1985).
[17] A different model was due to G.S. Bales and A. Zangwill, Ref. [11]; and J. Vac. Sci. Technol. A **9**, 145 (1991), where only the normal component of the incident flux is taken into account.
[18] For the data presented here, more than 2000 CPU hours were spent on a SiliconGraphics workstation.
[19] The width $W(t)$ can be fitted as $W(t) \sim t^{\beta}$ with $\beta = 1.0 \pm 0.04$ after the initial transients. See Fig. 2.
[20] In $1+1$ dimensions the coefficient α in Eq. (5) has a value 0.59 which leads to a larger value of the marginal wave number k_c than that of the $2+1$ situation; see Ref. [8].